Critical role of endothelial P-selectin glycoprotein ligand 1 in chronic murine ileitis

Jesús Rivera-Nieves,[1,4] Tracy L. Burcin,[2,3] Timothy S. Olson,[4] Margaret A. Morris,[2,3] Marcia McDuffie,[4,5] Fabio Cominelli,[1,4] and Klaus Ley[2,3,6]

[1]Digestive Health Center of Excellence, [2]Robert M. Berne Cardiovascular Research Center, [3]Department of Biomedical Engineering, [4]Internal Medicine, [5]Microbiology and [6]Molecular Physiology and Biological Physics, University of Virginia Health Sciences Center, Charlottesville, VA 22908

L-selectin ligands might be relevant for inflammatory cell trafficking into the small intestine in a spontaneous model of chronic ileitis (i.e., SAMP1/YitFc mice). Immunoblockade of peripheral node addressin or mucosal addressin cell adhesion molecule 1 failed to ameliorate ileitis, whereas P-selectin glycoprotein ligand 1 (PSGL-1) neutralization attenuated both the adoptively transferred and spontaneous disease. PSGL-1 was detected in venules of mesenteric lymph node and small intestine by immunohistochemistry and confirmed by real-time reverse transcription polymerase chain reaction and flow cytometry. In addition, reconstitution of wild-type mice with PSGL-1$^{-/-}$ bone marrow demonstrated that PSGL-1 messenger RNA and PSGL-1 protein expression remained on endothelium, localized within mesenteric lymph node and small intestine. Endothelial PSGL-1 bound P-selectin–IgG and its blockade or genetic deletion altered the recruitment of lymphocytes to the small intestine, as revealed by intravital microscopy and homing studies. Endothelial expression of PSGL-1 adds a new dimension to the various cellular interactions involved in small intestinal recruitment. Thus, the multiple roles of PSGL-1 may explain why targeting this single adhesion molecule results in attenuation of chronic murine ileitis, a disease previously resistant to antiadhesion molecule strategies.

CORRESPONDENCE
Jesús Rivera-Nieves:
jr3u@virginia.edu

Abbreviations used: CD, Crohn's disease; FSC, forward light scatter; HEV, high endothelial venule; HRP, horseradish peroxidase; LP, lamina propria; MAdCAM-1, mucosal addressin cell adhesion molecule; MLN, mesenteric lymph node; PNAd, peripheral node addressin; PSGL-1, P-selectin glycoprotein ligand 1; SSC, side light scatter; UC, ulcerative colitis.

The inflammatory bowel diseases (ulcerative colitis [UC] and Crohn's disease [CD]) are chronic immune-mediated conditions that affect more than one million patients in North America and lead to more than $3.6 billion in productivity losses each year (1, 2). The inflammatory process is characterized by heavy leukocytic infiltration of the intestinal lamina propria (LP), leading to fibrosis and loss of function (3, 4). Although the etiology of the disease remains mostly unknown, modulation of the immune response by immunomodulators (e.g., azathioprine, 6-mercaptopurine), corticosteroids, and mAbs to TNF-α improve disease symptoms and outcomes (3–6). Although UC affects strictly the large intestine, CD primarily involves the small intestine, predominantly the terminal ileum (chronic ileitis) (3, 4). Thus, the recirculating lymphocyte pool likely possesses a defined repertoire of adhesion molecules and chemokines ("address code") (7) that allows them to distinguish between the small and large intestine. However, the specific combination of molecules engaged by pathogenic cells to localize specifically to the small intestine has not been identified.

The recent characterization of mouse models that spontaneously develops chronic ileitis (i.e., the SAMP1/Yit and SAMP1/YitFc models) enabled us to study the trafficking pathways into the chronically inflamed small intestine (8–10). SAMP1/YitFc mice develop discontinuous, transmural chronic inflammation localized to the small intestine (8, 9) that closely recapitulates the human disease (10, 11). The LP is intensely infiltrated by effector T cells, which display an activated phenotype and adoptively transfer disease to SCID mice (9). However, unlike the CD45RB^{high} transfer model (12), lymphocytes from SAMP1/YitFc mice predominantly induce ileitis and not colitis, suggesting an inherent capacity to recirculate

The online version of this article contains supplemental material.

preferentially to the small intestine (9). The resulting ileitis is also resistant to modulation by regulatory cells as cotransfer of CD45RB^{low} or CD25$^+$ T cells, which abolishes colitis and has no effect on ileitis (13). In addition, although colitis responds to single adhesion molecule blockade (14–17), ileitis requires interference with two or more adhesion pathways (i.e., ICAM-1/VCAM-1, L-selectin/mucosal addressin cell adhesion molecule-1 [MAdCAM-1], α_4 integrins) (18, 19). This is in keeping with clinical trials in which patients with CD receiving natalizumab (a mAb that targets the shared α_4 moiety of both $\alpha_4\beta_7$ and $\alpha_4\beta_1$ integrins) achieved a clinical response, whereas specific blockade of the gut-homing integrin $\alpha_4\beta_7$ was not more efficacious than the placebo (20–22).

Gut-homing CD4$^+$ T cells from SAMP1/YitFc mice coexpress not only $\alpha_4\beta_7$ and $\alpha_4\beta_1$ integrins, but also L-selectin (19). This L-selectin^{hi} population produces copious amounts of TNF-α and plays an important role in disease induction in SCID mice (19). L-selectin is involved in trafficking of naive and subpopulations of memory CD4$^+$ T cells to intestinal sites (19, 23, 24), but the small intestinal endothelial L-selectin ligands are not known. Identification of endothelial ligands that may be preferentially used in inflammatory trafficking may prove valuable for the development of therapeutic agents, as L-selectin is ubiquitously expressed.

Specialized endothelial cells express glycoproteins that serve as L-selectin ligands in secondary lymphoid organs, including a heterogeneous group of glycans that share the peripheral node addressin (PNAd) epitope (25, 26). MAdCAM-1 (the endothelial ligand for $\alpha_4\beta_7$ integrin) is present in intestinal- and gastrointestinal-associated lymphoid tissues (27) and can also serve as an L-selectin ligand when appropriately glycosylated (28). P-selectin glycoprotein ligand 1 (PSGL-1) (29) can also bind L-selectin (expressed on most leukocytes), P-selectin (expressed on inflamed endothelial cells and activated platelets), and E-selectin (expressed on inflamed endothelial cells) (30, 31).

The potential role of L-selectin in trafficking to the inflamed small intestine prompted us to search for its associated intestinal endothelial ligands. A monoclonal antibody against PSGL-1, but not any other single antiadhesion molecule strategy, attenuated both the CD4$^+$-induced and the spontaneous ileitis. Unexpectedly, not only the infiltrating leukocytes, but also endothelial cells from small intestine and mesenteric lymph node (MLN) expressed functional PSGL-1. Our results, therefore, suggest that PSGL-1 is an integral part of the address code for small intestinal homing and that it is critically involved in recruitment of leukocytes, including effector CD4$^+$ T cells, into the LP of the chronically inflamed small intestine.

RESULTS

PSGL-1 plays a critical role in chronic murine ileitis

We have recently shown that L-selectin plays an important role in adoptively transferred chronic ileitis (19), a disease induced by pathogenic CD4$^+$ T cells (9). To identify relevant L-selectin ligands within the microcirculation of the terminal ileum, we designed a series of therapeutic studies. SCID mice adoptively transferred with CD4$^+$ T cells isolated from donor SAMP1/YitFc mice develop severe ileitis within 6 wk (9, 18). The PNAd epitope (shared by several L-selectin ligands) was expressed within the MLN of inflamed SCID mice, but not in those from their noninflamed counterparts (Fig. 1 A). Therefore, 6 wk after adoptive transfer, we targeted PNAd using the mAb MECA-79 alone (not depicted) or in combination with anti–MAdCAM-1 (MECA-367) for 3 d (Fig. 1 B) to determine whether PNAd was the critical small intestinal endothelial ligand. This treatment provided no therapeutic benefit (active index = 4.5 ± 0.7, chronic index = 4.4 ± 0.9) compared with mice treated with isotype antibodies (active index = 4.1 ± 0.6, chronic index = 4.9 ± 0.6).

MAdCAM-1 serves as a ligand for $\alpha_4\beta_7$ integrin and for L-selectin when appropriately glycosylated (27, 28). The mAb MECA-367 interferes with $\alpha_4\beta_7$ binding, whereas MECA-89 blocks interactions with L-selectin (32). However, MAdCAM-1

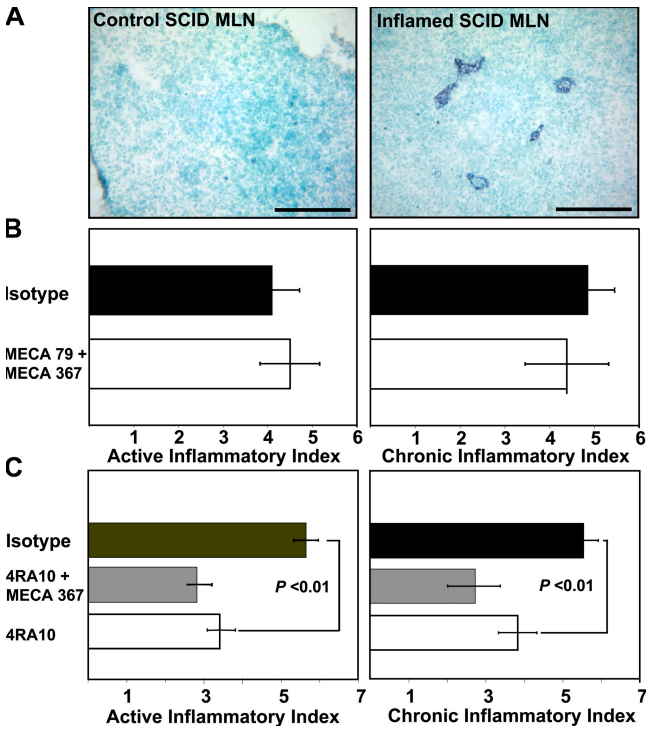

Figure 1. Peripheral node adressin (PNAd) expression and blockade in adoptively transferred ileitis. (A) Immunohistochemistry was performed on frozen sections before (left) and 6 wk after transfer (right) as per the description in Materials and methods. PNAd expression was detected in MLN HEVs (right) of SCID mice with chronic ileitis, but not before adoptive transfer (left). Representative micrographs from tissues obtained from three mice before and after transfer are shown. Bars, 100 μm. (B and C) The effect of antibody blockade on inflammatory indices. (B) Inflamed SCID mice were treated with isotype mAb (n = 12), with anti-PNAd/anti–MAdCAM-1 antibodies combined (MECA-79 + MECA 367, n = 10) or (C) with isotype mAb (n = 8), with anti–MAdCAM-1/anti–PSGL-1 antibodies combined (4RA10 + MECA 367, n = 7), or with anti–PSGL-1 antibody (4RA10, n = 7). Error bars show the mean ± SEM from four independent experiments.

does not appear to be the critical small intestinal endothelial ligand, as there was no therapeutic benefit after MECA-89 antibody treatment alone or when combined with MECA-367 (active index = 4.8 ± 0.7, chronic index = 5.7 ± 0.7) compared with isotype-treated controls (active index = 5.3 ± 0.8, chronic index = 5.2 ± 0.9) (unpublished data).

We tested whether PSGL-1, a known pan-selectin ligand, could be the endothelial counterpart responsible for the therapeutic effect of L-selectin blockade. Using the function-blocking mAb 4RA10 (33), we targeted PSGL-1 alone or combined with anti–MAdCAM-1 mAb MECA-367 in inflamed SCID mice. Animals were administered three doses of mAb/s every other day, 6 wk after adoptive transfer, as the ileitis reached maximum severity. 4RA10 reduced both active and chronic inflammatory indices (active index = 3.4 ± 0.4, chronic index = 3.8 ± 0.5) compared with isotype-treated controls (active index = 5.6 ± 0.3, chronic index = 5.5 ± 0.4, $P < 0.01$) (Fig. 1 C). Additional MAdCAM-1 blockade did not significantly improve the effect (4RA10/MECA 367; active index = 2.8 ± 0.4, chronic index = 2.7 ± 0.6; the p-value vs. 4RA10 was not significant).

PSGL-1 blockade attenuated spontaneous chronic ileitis

To investigate whether a similar therapeutic effect could be achieved on the spontaneous ileitis of SAMP1/YitFc mice, we administered three doses of the 4RA10 mAb (200 μg) every other day to 10-wk-old mice, which at that age exhibit robust ileitis. Prior studies had shown that, at this time point, the disease is refractory to all antiadhesion strategies evaluated (18). However, 4RA10 reduced the villous distortion index by 30% ($P < 0.005$) (Fig. 2 A), the active inflammatory index (granulocytic infiltrates) by 70% ($P < 0.0001$) (Fig. 2 B), and the chronic inflammatory index (lymphocytic/monocytic infiltrates) by 50% ($P < 0.0005$) (Fig. 2 C) compared with isotype-treated controls (Fig. 2, black bars). The total inflammatory index was reduced by 50% ($P < 0.0001$) (Fig. 2 D) and restoration of the villous and crypt architectures was also observed in the 4RA10-treated mice (Fig. 2, E and F). No other single or combined antiadhesion molecule strategy has shown comparable therapeutic benefit (18). The therapeutic effect of anti–PSGL-1 mAb in SAMP1/Yit mice has been independently verified by Inoue et al. (34).

PSGL-1 expression increased on activated effector CD4$^+$ T cells from SAMP1/YitFc mice

To identify potential cellular targets for PSGL-1 immunoblockade, we investigated whether expression of PSGL-1 or its reactivity to P-selectin were affected by the chronic inflammatory process. Flow cytometric analyses of MLN cells demonstrated a significantly higher percentage of activated CD44^{high} cells in SAMP1/YitFc mice compared with noninflamed AKR mice ($P < 0.01$) (Fig. 3 A), whereas essentially all MLN CD4$^+$ T cells from both strains expressed PSGL-1. In contrast, although only 1.3% of uninflamed AKR CD4$^+$/CD44^{high} MLN cells bound P-selectin–IgG, this fraction increased to 7% in inflamed SAMP1/YitFc mice ($P < 0.001$)

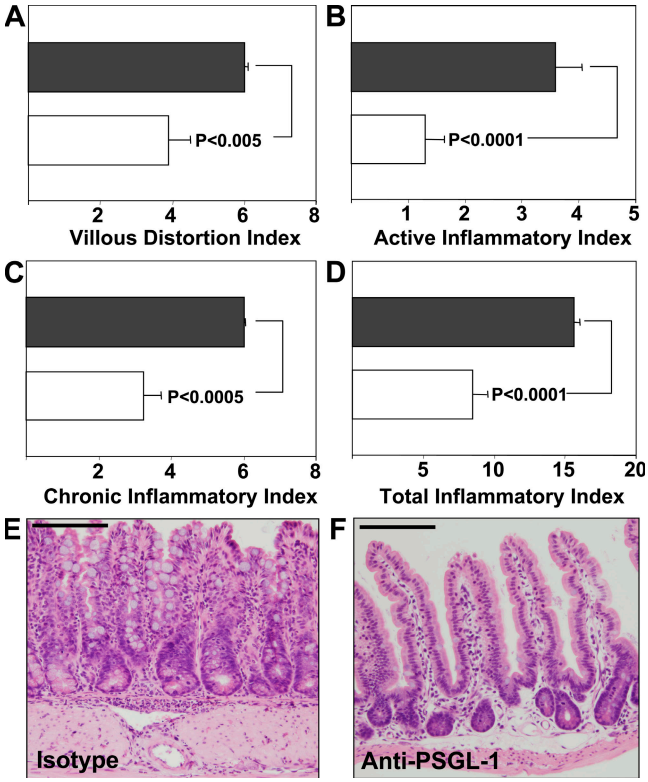

Figure 2. Anti–PSGL-1 antibody attenuates ileitis in SAMP1/YitFc mice. (A–D) Mice were injected with isotype mAb (black bars, $n = 12$) or with and anti–PSGL-1 antibody (4RA10) (white bars, $n = 10$), ileal tissues were harvested, and inflammatory indices were determined as described in Materials and methods. Error bars show the mean ± SEM from two independent experiments. (E and F) The effect of indicated treatment on intestinal architecture (representative micrographs, hematoxylin and eosin). Bars, 150 and 200 μm, respectively.

(Fig. 3 B), consistent with regulation of PSGL-1 function at the posttranslational level. The majority of the P-selectin–binding CD4$^+$ T cells were found within the CD44^{high}–activated population. The addition of 5 mM EDTA abolished selectin binding in both strains (unpublished data).

Leukocyte PSGL-1 is not required for the development of ileitis

Prior studies suggested that monocyte-expressed PSGL-1 was the critical element in the attenuation of ileitis achieved by anti–PSGL-1 treatment in SAMP1/Yit mice (34). To ascertain whether leukocyte PSGL-1 was required for the development of ileitis, we generated bone marrow chimeric SAMP1.B6MHC mice reconstituted with PSGL-1–sufficient (C57BL/6J, WTBM) or PSGL-1–deficient bone marrow. In this SAMP1 congenic substrain, the MHC originates from C57/BL/6J mice, allowing bone marrow transplantation from PSGL-1$^{-/-}$ mice on C57/BL6/J background. The mixed genetic background of native SAMP1/YitFc mice precludes such manipulation as the result of MHC mismatch. Heterozygous and homozygous Chr 17 congenics did not

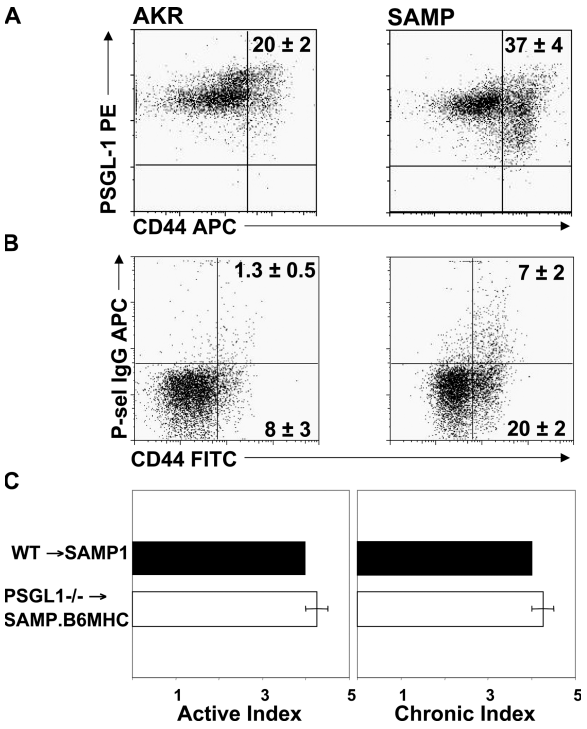

Figure 3. A higher percentage of SAMP1/YitFc (SAMP) CD4$^+$/CD44^{high} MLN cells bind P-selectin–IgG compared with cells from uninflamed AKR control mice (AKR). (A) PSGL-1 expression and (B) P-sel–IgG binding to MLN cells were analyzed by flow cytometry and gated on forward light scatter (FSC), side light scatter (SSC), and CD4. Representative data obtained from four and three mice, respectively. (C) The severity of ileitis was determined in SAMP1.B6MHC mice reconstituted with PSGL-1–sufficient (WT) or deficient (PSGL$^{-/-}$) bone marrow. Error bars show the mean ± SEM.

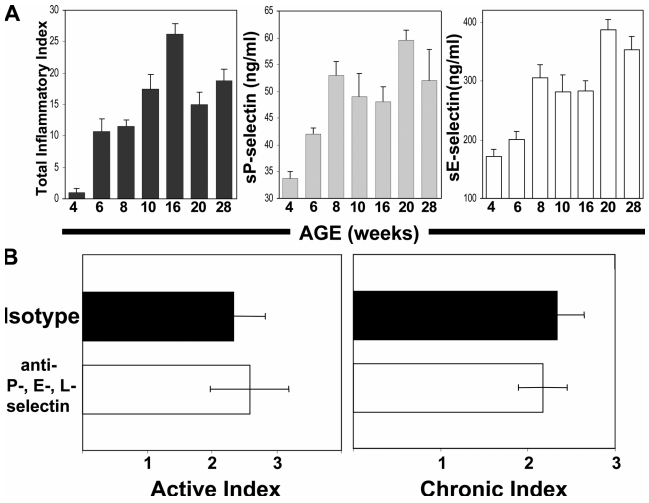

Figure 4. Soluble serum P- and E-selectin levels were elevated in inflamed SAMP1/YitFc mice but pan-selectin antagonism is not solely responsible for the effect of PSGL-1 immunoblockade. (A) The severity of ileitis (left) and the serum levels of soluble P- and E-selectins (middle and right) were determined in SAMP1/YitFc mice as the disease progressed (mean ± SEM, $n = 5$ mice/time point). (B) SAMP1/YitFc mice at 10 wk of age received antibodies against P-, E-, and L-selectins (mAb RB40.34, 9A9, MEL-14) or their respective isotype antibodies combined and the severity of the ileitis was assessed as described. Error bars show the mean ± SEM; $n = 7$ mice/treatment group.

differ from the parental SAMP1/YitFc strain in their cumulative incidence, kinetics, or severity of ileitis (median total ileitis score: SAMP = 9.8, SAMP.B6-MHC = 10.5; $n = 13$ and 24, respectively); therefore, neither the MHC nor other loci on Chr 17 regulate disease susceptibility (35). The disease of SAMP1.B6MHC mice reconstituted with PSGL-1–deficient bone marrow was indistinguishable from that of mice reconstituted with PSGL-1–sufficient bone marrow, suggesting that leukocyte-expressed PSGL-1 was not required for the development of ileitis.

Levels of soluble P- and E-selectins increased in inflamed SAMP1/YitFc mice, but pan-selectin antagonism did not attenuate chronic ileitis

Pan-selectin antagonism through targeted blockade of PSGL-1 (a pan-selectin ligand) is an obvious potential mechanism for the therapeutic effect of 4RA10. Therefore, we first examined whether P- and E-selectins played a role in the development of ileitis by measuring the levels of soluble selectins in serum as the disease progressed from 4 to 28 wk. Both soluble P- and E-selectin levels increased from 4 to 8 wk during the early stages of the disease and reached a plateau thereafter (Fig. 4 A). This correlation between soluble serum selectin levels and severity of inflammation supported a role for both P- and E-selectins in the development of the disease and justified a therapeutic study in which all selectins were simultaneously targeted. However, targeting all three selectins in 10-wk-old SAMP1/YitFc mice offered no therapeutic benefit (Fig. 4 B), suggesting that pan-selectin antagonism was not the sole mechanism of the disease-attenuating effect of mAb 4RA10.

Small intestinal endothelial cells express PSGL-1

We conducted immunohistochemical studies to determine whether the frequency of PSGL-1–expressing leukocytes increased with the inflammatory infiltrates of the chronically inflamed small intestine. Unexpectedly, PSGL-1 immunoreactivity was not only observed on hematopoietic cells but also on microvessels within the small intestinal villi and submucosa of inflamed adoptively transferred SCID mice (AT SCID, Fig. 5), as well as in terminal ileal microvessels of SAMP1/YitFc mice with chronic ileitis (Fig. 5). Because many of these vessels were located within inflamed sites, we conducted additional experiments to determine whether inflammation was required. PSGL-1 expression was similarly found on microvessels of noninflamed AKR mice, which do not develop ileitis, (Fig. 5) but not in PSGL-1–deficient mice or in mice that received an isotype-matched nonspecific antibody, followed by a secondary antibody (anti–rat horseradish peroxidase [HRP] conjugate). To exclude leukocyte fragment-derived PSGL-1 (36) as the source for the endothelial

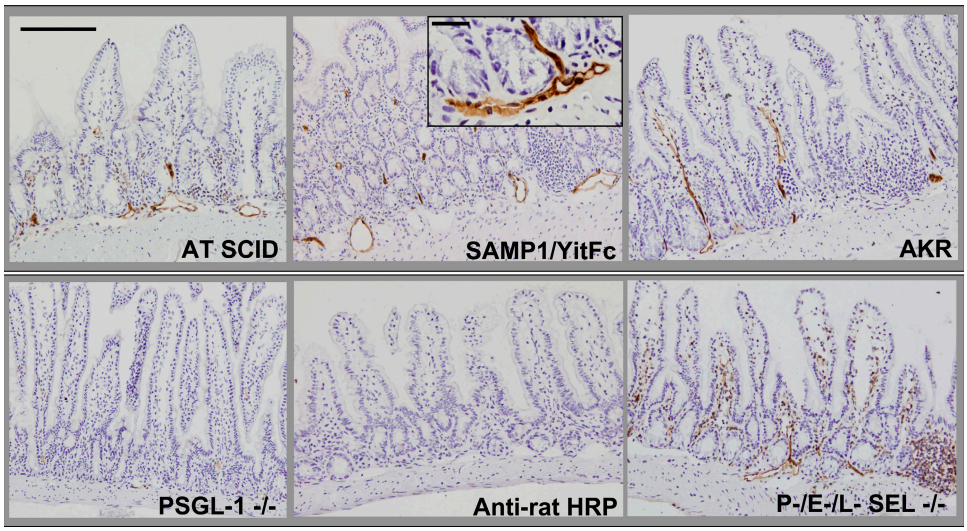

Figure 5. Small intestinal endothelial cells express PSGL-1. Immunohistochemistry was performed on frozen terminal ileal sections from the indicated mouse strains as per Materials and methods. PSGL-1 expression was detected on leukocytes and in venules within the LP and submucosa of adoptively transferred SCID mice (AT SCID), SAMP1/YitFc, and AKR mice. Minimal or no expression was observed in PSGL-1–deficient (−/−) mice or in AKR ileum reacted with anti-rat HRP after isotype antibody injection (Anti-rat HRP), whereas robust expression was seen in P-, E-, L-selectin triple-deficient (−/−) mice, which lack rolling leukocytes. Bar, 200 μm. Inset, high power of SAMP1/YitFc submucosal venules. Bar, 20 μm.

signal, we tested mice that lack P-, E-, and L-selectins (37). Leukocytes from these mice are expected to show little or no leukocyte rolling, limiting leukocyte-derived PSGL-1 deposition. However, P-, E-, L-selectin–deficient mice similarly showed robust endothelial PSGL-1 expression (Fig. 5).

Endothelial PSGL-1 binds P-selectin

To confirm endothelial PSGL-1 expression and function at the single cell level, we obtained ileal LP mononuclear cells by collagenase digestion, followed by a 2-h incubation at 37°C and staining of the adherent population for CD31, a pan-endothelial cell marker. Leukocytes were further depleted magnetically, removing cells that expressed CD45, a pan-leukocyte marker (Fig. 6 A) (38). 34% of the $CD45^{neg}/CD31^{pos}$ cells expressed PSGL-1 (Fig. 6 B), consistent with PSGL-1 expression in venules, which account for approximately one third of all microvascular endothelial cells. The same percentage of ileal endothelial cells was able to bind P-selectin–IgG (Fig. 6 C), but not a control human IgG chimera (not depicted), demonstrating that the endothelium-expressed PSGL-1 was functional. To directly demonstrate the expression of PSGL-1 message by endothelial cells, mRNA was extracted from a cellular fraction magnetically depleted of $CD45^{+}$ cells (98% $CD45^{neg}$), followed by further purification $CD45^{neg}/CD31^{pos}$ small intestinal endothelial cells using FACS sorting. The presence of PSGL-1 mRNA was subsequently confirmed by real-time RT-PCR (unpublished data).

PSGL-1 mRNA expression localized to the small intestine and MLN of PSGL-$1^{-/-}$→WT bone marrow chimeric mice

To quantitatively measure PSGL-1 mRNA in situ and to determine whether PSGL-1 expression localized to specific tissues, we generated bone marrow chimeric mice through reconstitution of lethally irradiated wild-type C57BL/6J mice with bone marrow progenitors from PSGL-$1^{-/-}$ mice (31). PSGL-$1^{-/-}$→WT chimeric mice lacked leukocyte-derived PSGL-1(Fig. 7 A), but continued to express PSGL-1 within small intestinal endothelium (Fig. 7 B). Real-time RT-PCR of PSGL-$1^{-/-}$→WT chimeric mice tissues localized PSGL-1 mRNA within the duodenum, jejunum, ileum, and MLN but not within the kidney, spleen, liver, bone marrow, or heart. Peripheral blood leukocytes from control mice reconstituted with wild-type bone marrow (WT→WT) expressed PSGL-1 on leukocytes (Fig. 7 A), as well as PSGL-1 mRNA in all organs surveyed, commensurate with their leukocyte

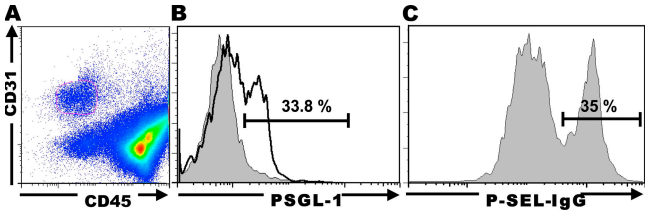

Figure 6. Primary intestinal endothelial cell PSGL-1 expression and reactivity with P-sel-IgG chimera. (A). LP mononuclear cells were obtained from terminal ilea of SAMP1/YitFc mice and plated for 2 h at 37°C. Adherent cells were recovered and stained for three color flow cytometry as per Materials and methods. Cells were gated on FSC, SSC, $CD45^{neg}$, $CD31^{+}$. (B) PSGL-1 expression was determined within the $CD45^{neg}$, $CD31^{+}$ gated cells (unshaded histogram) and compared with cells stained with isotype mAb control (shaded histogram). (C) Reactivity with P-sel-IgG chimera was determined in $CD45^{neg}$, $CD31^{+}$ gated cells. Representative data from four (A and B) and two (C) independent experiments, respectively, are shown.

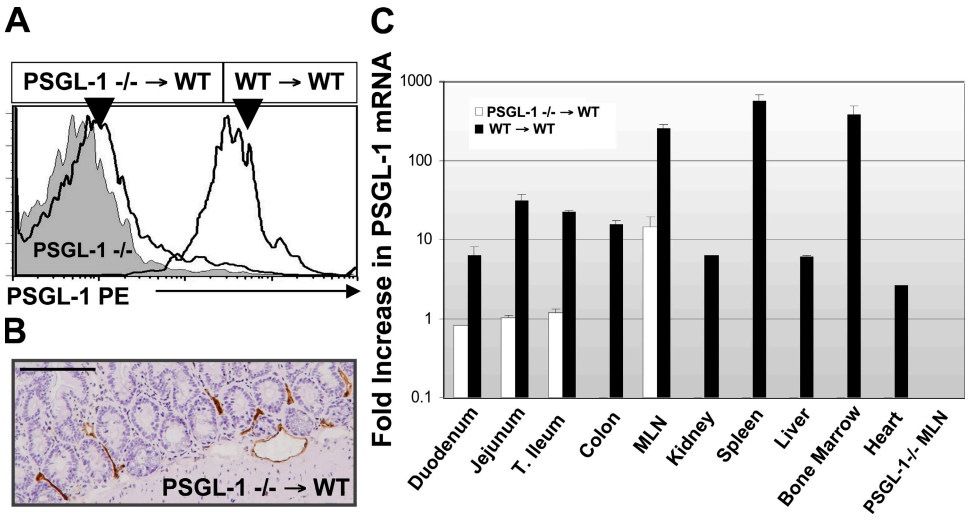

Figure 7. Endothelial PSGL-1 expression localized to the small intestine and MLN of PSGL1$^{-/-}$ → WT bone marrow chimeric mice. (A) Peripheral blood leukocytes from PSGL-1–deficient or indicated bone marrow chimeric mice were incubated with PE anti–PSGL-1 (2PH1) antibody as per Materials and methods. Cells were gated on FSC, SSC, and CD3. (B) Endothelial PSGL-1 was detected by immunohistochemistry in mice reconstituted with PSGL-1–deficient bone marrow using mAb 4RA10. Bar, 150 μm. (C) PSGL-1 mRNA levels from indicated organs of bone marrow chimeric and PSGL1$^{-/-}$ mice. Indicated tissues were harvested, RNA was obtained, and real-time RT-PCR was performed as per Materials and methods. Representative histograms, tissues, and mRNA expression were obtained from at least four bone marrow chimeric mice per group and run in triplicate. Error bars show the mean ± SEM.

content (Fig. 7 C, black bars). PSGL-1$^{-/-}$ tissues, used as negative control, lacked PSGL-1 mRNA (representative PSGL-1$^{-/-}$ MLN shown, Fig. 7 C). Collectively, these data demonstrate that venular endothelial cells in the small intestine and MLN express functional PSGL-1.

Functional significance of endothelial PSGL-1 for lymphocyte recruitment

To examine the in vivo significance of endothelial PSGL-1 expression in the recruitment process to the small intestine, we performed homing assays and intravital microscopy. CD4$^+$/L-selectin$^+$ lymphocytes were enriched magnetically, radioactively labeled with chromium 51 and adoptively transferred into PSGL-1–sufficient (+/+) and –deficient (−/−) mice. To account for the possibility that chronic inflammation may be required for the posttranslational modifications that render endothelial PSGL-1 functional for small intestinal recruitment, we used PSGL-1–deficient and –sufficient TNFΔARE mice that, like SAMP1/YitFc mice, develop chronic ileitis (39). Decreased incorporation of radioactivity was observed throughout the small intestine and colon of PSGL-1–deficient TNFΔARE mice; however, these differences reached statistical significance only in the MLN and ileum ($P < 0.05$). No differences in recruitment were seen in the liver, kidney, or colon (Fig. 8).

Prior immunohistochemical studies have shown that the PSGL-1 signal was not exclusively present in villous and submucosal microvessels, but that some larger caliber vessels within the muscularis and serosa also expressed PSGL-1 (Fig. 9 A, arrow). Using intravital microscopy, we identified serosal venules of the terminal ileum in which rolling of fluorescently labeled cells could be visualized before and after injection of an anti–PSGL-1 mAb (4RA10). To exclude the possibility that a potential effect of the anti–PSGL-1 mAb could be mediated by interference with leukocyte PSGL-1, the injected cells originated from PSGL-1–deficient mice. Most of the observed rolling occurred in serosal vessels of ∼50–80 μm in diameter, where engaged cells (Fig. 9 B, red arrows) could be identified as they advanced much slower than their free-flowing counterparts (Fig. 9 B, blue arrowheads). A significant reduction in the number of rolling cells (∼70%) was observed after anti–PSGL-1 antibody injection (Fig. 9 C). As the rolling cells lacked PSGL-1, the effect of the antibody must be attributed to interference with endothelial PSGL-1 interactions.

DISCUSSION

L-selectin ligands are expressed at sites of chronic inflammation, including the small intestine of patients with CD (26), but their role in recruitment of L-selectin–expressing leukocytes directly into effector sites is incompletely understood (26). In this study, we demonstrate that the pan-selectin ligand PSGL-1 plays a critical role in ileitis, as the function-blocking antibody (4RA10) decreased granulocytic and lymphocytic infiltrates in both CD4$^+$-dependent and spontaneous murine ileitis. Moreover, we demonstrate that small intestinal high endothelial venule (HEV)-like vessels express functional PSGL-1. Its immunoblockade results in decreased rolling leukocytes, decreased recruitment of CD4$^+$ T cells to the terminal ileum, and attenuated ileitis. Our results provide evidence that PSGL-1 is part of the address code for small intestinal trafficking.

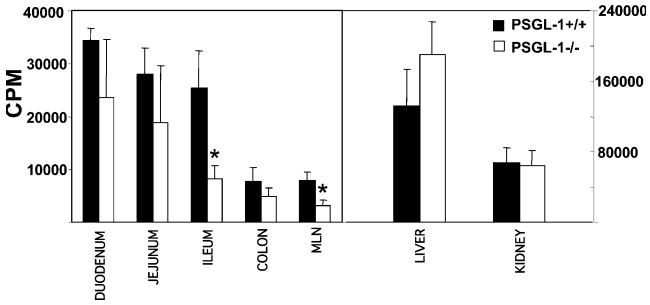

Figure 8. Homing of CD4$^+$ T cells to the terminal ileum is impaired in PSGL-1–deficient mice. Chromium 51–labeled L-selectin$^+$ CD4 T cells were injected into PSGL-1–sufficient (+/+) and –deficient (−/−) TNFΔARE mice as per Materials and methods. Radioactivity was determined in the aforementioned organs 72 h after cell transfer. Error bars show the mean ± SEM from three mice/experimental group. *, $P < 0.05$.

The mAb MECA-79 recognizes several sialomucins (PNAd) that, when properly glycosylated, serve as L-selectin ligands. Functionally, MECA-79 blocks lymphocyte interactions with HEVs in vitro and short-term lymphocyte homing to lymph nodes in vivo (25). Its role in inflammatory trafficking has been shown in the inflamed pancreas (40, 41) and lacrimal glands (42). MECA-79 binds to HEV-like vessels in the organized lymphoid aggregates present in chronically inflamed tissues (26). Although we demonstrate PNAd expression in SCID mice with ileitis, no beneficial therapeutic effect was seen by MECA-79 administration.

MAdCAM-1, the $\alpha_4\beta_7$ integrin endothelial ligand expressed in intestine and gastrointestinal-associated lymphoid tissues (27), serves as an L-selectin ligand when appropriately glycosylated (7, 27, 28). MAdCAM-1 is constitutively expressed in postcapillary venules of intestinal LP, MLN, and Peyer's patches HEVs (27, 43), and is aberrantly expressed in the inflamed pancreas (39). Furthermore, MAdCAM-1 is upregulated in the chronically inflamed small and large intestine of patients with UC and CD, where it is likely induced by TNF-α (43, 44). The mAb MECA-367 binds to the first Ig domain of MAdCAM-1 and interferes with $\alpha_4\beta_7$ binding, whereas MECA-89 binds to the second Ig domain, which interferes with L-selectin interactions as a result of its proximity to the mucinous portion of MAdCAM-1 (32). If MAdCAM-1 mediated critical L-selectin interactions in the gut, we would expect that combined MECA-367/MECA-89 treatment would provide the same benefit as combined MECA-367/MEL-14 (19). However, administering MECA-89 together with MECA-367 provided no added therapeutic benefit.

PSGL-1 binds to L-selectin (29), E-selectin, and P-selectin (30, 31). The most comprehensive survey of PSGL-1 expression to date identified bone marrow–derived cells as the primary site of expression, whereas expression by endothelial cells was limited to small venules and capillaries of pathological tissues (i.e., benign prostatic hypertrophy and fibrocystic disease of the breast) (45). PSGL-1 binding to selectins is regulated by fucosyltransferases, core 2-glucosaminyltransferases, sialyltransferases, and sulfotransferases, which are constitutively expressed in myeloid cells but regulated in lymphocytes.

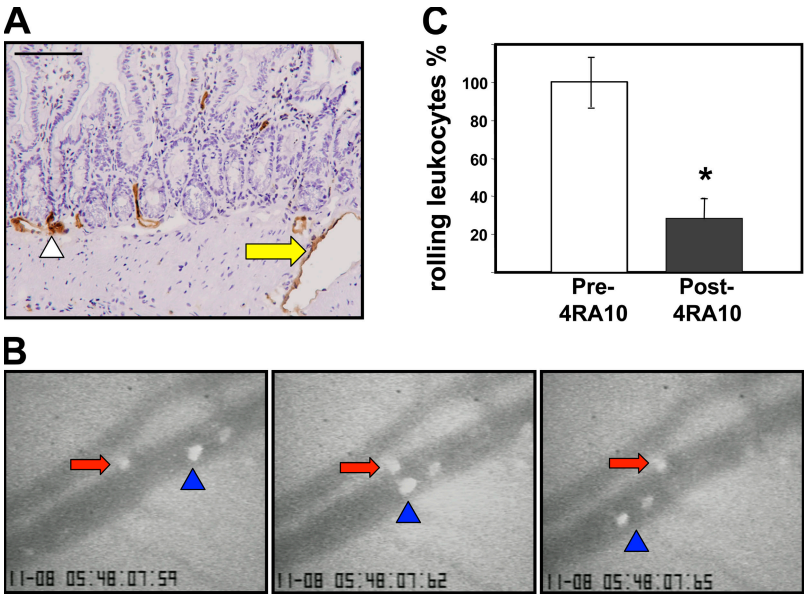

Figure 9. PSGL-1 blockade decreased splenocyte–endothelial interactions in the small intestinal vasculature. (A) Endothelial PSGL-1 signal was observed in small (arrowhead) and large vessels (yellow arrow) within the small intestinal muscularis and serosa. The larger serosal vessels were monitored via intravital microscopy. Bar, 200 μm. (B) Rolling CFSE-labeled PSGL-1–deficient cells (red arrows) proceed much slower than cells not interacting with wild-type vessels (blue arrowhead) before (B) PSGL-1 blockade. (C) A significant decrease in the number of rolling cells was observed after injection of 4RA10 (percent of normalized total rolling cells [error bars show the mean ± SD] before and after 4RA10 injection from four experiments in which one to three vessels/mouse were monitored; *, $P < 0.05$).

Thus, effector memory cells of the Th1 type bind selectins better than Th2 polarized $CD4^+$ T cells (30, 46–48). Endothelial cells also express most, if not all, of these glycosyltransferases (49), suggesting that all of the machinery necessary to express functional selectin binding activity is present.

Different from other models of colitis that may be successfully treated by blockade of single adhesion molecules (14–17), the spontaneous chronic ileitis of SAMP/Yit mice is refractory to single and to many combined antiadhesion molecule strategies (i.e., MAdCAM-1, $\alpha_4\beta_7$ integrin, ICAM-1, VCAM-1, α_4 integrin, combined ICAM-1/VCAM-1, and ICAM-1/α_4) (18). In contrast, the current data shows that targeting PSGL-1 alone ameliorates ileitis. This effect cannot be solely explained by the expected pan-selectin antagonism as combined blockade of all three selectins failed to attenuate ileitis. Expression of PSGL-1 on ileal endothelium provides a plausible explanation of why blockade of a single adhesion molecule is effective. First, PSGL-1 blockade prevents entry of functional PSGL-1–expressing (Th1-polarized) (30, 46–48) and L-selectin–expressing (naive and subpopulations of memory $CD4^+$ T cells) into MLN and ileal LP (19, 23), where endothelial PSGL-1 acts as an "addressin" for small intestinal homing of L-selectin–expressing cells. Second, anti–PSGL-1 interferes with recruitment of $PSGL\text{-}1^+$ granulocytes and monocytes, as well as those expressing L-selectin, which might use endothelial PSGL-1 as a ligand. Third, blocking PSGL-1 prevents secondary leukocyte tethering to P-selectin on adherent platelets, as well as PSGL-1/P-selectin- and/or PSGL-1/L-selectin–mediated leukocyte–leukocyte and leukocyte–platelet interactions. P-selectin–PSGL-1 interactions are known to exacerbate atherosclerosis (50) and dextran sulfate sodium–induced colitis (51). Ligation of PSGL-1 on activated Th1 cells may also induce rapid apoptosis of these cells, which are known to be pivotal for induction and maintenance of ileitis (52).

Collectively, our data demonstrate that PSGL-1 is constitutively expressed on endothelial cells of the MLN and small intestine. In this location, endothelial PSGL-1 may act as an addressin to support homing of L-selectin–expressing leukocytes and memory T cells into the small intestinal LP and MLN. Because the SAMP1/YitFc model shares many features of the human disease, it would be reasonable to expect that PSGL-1 may represent a viable therapeutic target for the treatment of patients with CD.

MATERIALS AND METHODS

Mice. SAMP1/YitFc mice were generated by brother–sister matings for >30 generations from two breeding pairs provided by S. Matsumoto (Yakult Institute for Microbiological Research, Tokyo, Japan) and kept under specific pathogen-free conditions at the University of Virginia (9, 10). As most identifiable genes were AKR derived, age-matched AKR/J mice were used as controls (35). Fecal samples from SAMP1/YitFc mice were consistently negative for *Helicobacter hepaticus*, *Helicobacter bilis*, and other mouse *Helicobacter* species, as well as for protozoa and helminthes.

C3SnSmn.CB17-$Prkdc^{scid}$/J SCID mice (6–8 wk old) (The Jackson Laboratory) were purchased and housed at the University of Virginia vivarium under specific pathogen-free conditions for 1 wk before SAMP1/YitFc $CD4^+$ T cell adoptive transfer and thereafter. $PSGL\text{-}1^{-/-}$ and E-, P-, L-selectin–deficient mice, both on C57BL/6 background were generated as described previously (31, 37).

TNFΔARE mice were generated as described previously (39), backcrossed to C57BL/6J mice (18 generations), and kept under specific pathogen-free conditions. The C57BL/6J genetic background did not alter the localization, time course, or severity the intestinal inflammation (unpublished data). $TNF\Delta ARE^{+/-}/PSGL\text{-}1^{-/-}$ were generated by crossing $TNF\Delta ARE^{+/-}$ mice to $PSGL\text{-}1^{-/-}$ mice. The double mutant mice were obtained after two backcrosses. PSGL-1 deficiency was confirmed by PCR and flow cytometry of peripheral leukocytes.

SAMP.B6-MHC congenic mice for alleles from the C57BL/6J (B6) chromosome 17 were generated by introgression of a B6 interval defined by the microsatellite loci D17Mit16 (31.3 Mb) and D17Mit221 (87.9 Mb) onto the SAMP genetic background using a marker-assisted selection ("speed congenic") protocol. This interval included the entire major histocompatibility complex, converting the new congenic strain to the H-2b haplotype from H-2k. This change renders SAMP.B6-MHC congenic mice as suitable recipients for bone marrow from C57BL/6J (B6) mice and $PSGL\text{-}1^{-/-}$ mice on this background, without altering the intestinal phenotype (35). All animal handling procedures were approved by the University of Virginia Health Sciences Center institutional committee for animal use.

Tissue collection and histological analyses. Mice were anesthetized and killed at the times required by the experimental design. The MLN was identified at the confluence of the mesenteric vasculature and harvested. The distal ilea (10 cm) were resected, opened, rinsed of debris, oriented from distal to proximal, and pinned longitudinally in corkboard. Tissues were fixed in 10% buffered formalin or Bouin's, embedded in paraffin, and cut into 3–5 μm sections. Resulting sections were stained with hematoxylin and eosin. Histological assessment of ileal inflammation was performed by a single pathologist in a blinded fashion using a standardized semi-quantitative scoring system as described previously (18).

Immunohistochemistry. Mice were injected with mAbs 4RA-10 against PSGL-1, MECA-79 against PNAd or isotype control mAb (IgG1, IgM, respectively) i.p. MLN and ilea were harvested 30 min after mAb injection and snap frozen, and sections (5 μm) were cut on a cryostat (Microm HM505N). Secondary staining was conducted with rabbit anti–rat antibody HRP using either VIP purple or DAB as substrates and methyl green or hematoxylin as counterstains, respectively (Vector Laboratories). Nonspecific binding was reduced using normal mouse serum (Sigma-Aldrich). Tissues from mice injected with isotype antibody served as controls.

Determination of serum soluble P- and E-selectin levels. Serum levels of soluble P- and E-selectins were determined by ELISA per the manufacturer's instructions from mice of the indicated ages (R&D Systems).

Intestinal LP lymphocyte and endothelial cell isolation. MLN were aseptically removed at the time of necropsy. Single cell suspensions were obtained by gently pressing the MLN against a 100-μm cell strainer. LP mononuclear cell isolation was performed as described previously (19).

Cell culture. For enrichment of adherent endothelial cells, LP mononuclear cells were cultured at 37°C in six-well flat-bottom plates at 10^6 cells/ml in complete medium (RPMI 1640 with 10% FBS, 2 mM L-glutamine and 1% penicillin/streptomycin) for 2 h or leukocytes were depleted using $CD45^+$ magnetic beads.

T cell and endothelial cell enrichment and separation. Enriched $CD4^+$ T cell fractions were obtained by incubation with anti-CD4–bound magnetic beads and sorted into discrete populations, using a magnetic cell–sorting system. Endothelial cell fractions were enriched by depleting the LP mononuclear cell fraction of $CD45^+$ cells using anti-CD45 magnetic beads (Miltenyi Biotec) following manufacturer's instructions. Flow cytometry confirmed 95–97% purity of $CD4^+$ T cell fractions and 98% purity of CD45 negative fraction, which was further purified by FACS sorting.

$CD4^+$ T cell adoptive transfer. SAMP1/YitFc (30–40 wk old) mice MLN were harvested and rendered into a single cell suspension, followed by positive selection for CD4 using magnetic beads. $CD4^+$ lymphocytes (10^5/mouse) were injected i.p. or i.v. into 6–8-wk-old SCID mice (The Jackson Laboratory). Neither the selection protocols (positive or negative) nor the route of injection (i.p. or i.v.) altered the severity or time course of disease. Mice were housed in a barrier facility and fed irradiated, standard chow. After 5 wk, the adoptively transferred mice showed ileitis with moderate to severe LP leukocyte infiltration and architectural changes (villous and crypt distortion, goblet cell hyperplasia, and hypertrophy of the muscularis propia).

In vivo homing. The in vivo migration of lymphocytes was analyzed as described previously (53). In brief, magnetically enriched $CD4^+/CD62L^+$ lymphocytes were labeled with 20 μCi chromium 51/ml. A total of 50×10^6 lymphocytes suspended in 0.5 ml were injected i.p. into 8–12-wk-old C57BL/6J ($n = 3$) or PSGL-$1^{-/-}$ mice ($n = 3$). Mice were killed after 72 h and the distribution of radioactivity in different organs was measured. Each sample was counted to 3% statistical error. The mean values and their standard error were determined from three animals per strain.

Flow cytometry and cell sorting. Fluorescently tagged monoclonal antibodies reactive with PSGL-1 (PE-labeled 2PH1; BD Biosciences) or P-sel human Ig-G chimera (2 μg/10^6 cells; BD Biosciences) or control CD4-human IgG chimera (2 μg/10^6 cells, a gift from J.B. Lowe, University of Michigan, Ann Arbor, MI) preincubated with allophycocyanin-labeled anti–human IgG Fab fragments (Zenon Human IgG labeling kit; Invitrogen) were subsequently incubated with cells in suspension for 20 min, including FITC-labeled anti-CD4 (GK1.5) for gating of MLN cells or PERCP anti-CD45 (30-F11) and FITC or allophycocyanin–anti-CD31 (390) (BD Biosciences) for gating of intestinal endothelial cells. Cells were fixed with 1% paraformaldehyde and three-to-four color analyses were performed using the FACS Calibur system (Becton Dickinson Immunocytometry Systems). Further analyses were performed using FLOWJo software (Tree Star Inc.). Endothelial cells were sorted using a FACSVantage sorter.

Real-time RT PCR. RT-PCR primers and Taqman probes were designed using Beacon Designer V3.0 software (Premier Biosoft). The primers were designed to amplify WT PSGL-1 mRNA but not mRNA from PSGL-$1^{-/-}$ mice (truncated protein). Total RNA was isolated using RNAeasy Mini-Kit (QIAGEN) with DNase treatment (Rnase-Free Dnase Kit; QIAGEN). Reverse transcription was performed using 500 ng of RNA with an Omniscript RT Kit (QIAGEN) and oligo-dT primers. The primers were tested for specificity by standard PCR using cDNA made from WT mice and PSGL-$1^{-/-}$ mice. Reaction conditions were optimized and 2 μL of sample cDNA was multiplexed with GAPDH and PSGL-1 primers on an iCycler iQ Real-Time Detection System (QIAGEN). Values were determined using the iCycler iQ Real-Time Detection System Software v3.0a (QIAGEN). The corresponding values were normalized to GAPDH. The PSGL-1 primers used were: forward 5′-CTTCCTTGTGCTGCTGACCAT-3′, reverse 5′-TCAGGGTCCTCAAAATCGTCATC-3′ and probe 5′-CCAACCAC-CTGCC TCCGTTCCCG-3′.

Therapeutic interventions. mAbs (200 μg each) against the following: PNAd (MECA-79, IgM), PSGL-1 (4RA-10, IgG1), MAdCAM-1 (MECA-367 or MECA 89, rat IgG 2a), P-selectin (RB40-34, IgG1), E-selectin (10E9.6, IgG2A), L-selectin (MEL-14, IgG2a), or irrelevant corresponding isotype control mAb were injected i.p. every other day for 3 d, 5 wk after adoptive transfer of SCID mice or at 10 wk of age for SAMP1/YitFc mice. Mice were killed 16–18 h after the last dose. MECA-367, MECA 79, and MECA-89 were obtained from the American Type Culture Collection. 4RA10 was obtained from D. Vestweber (University of Munster, Munster, Germany). Antibodies were produced and purified by HPLC from hybridoma supernatants at the University of Virginia Biomolecular Core Facility.

Generation of bone marrow chimeric mice. C57BL/6J bone marrow transplant recipients were irradiated twice with 600 rad before and 4–6 h after injection of donor cells. Bone marrow cells were harvested in RPMI 1640 containing 10% fetal calf serum. 7.5×10^6 cells/500 μl were injected into the tail veins of recipient mice. Mice were killed 6–10 wk after transplantation.

Intravital microscopy. C57BL/6J mice were prepared for intravital microscopy as per previously described methods (54). A 1.5-cm incision was made along the linea alba and the cecum and terminal ileum were exposed. The intestinal serosa was covered with plastic wrap and superfused with bicarbonate-buffered saline containing 100 nM isoproterenol. CFSE-labeled cells ($10–20 \times 10^6$/200 μl PBS) from PSGL-$1^{-/-}$ mice were injected through a jugular vein catheter and the serosal vessels in which rolling cells could be visualized by stroboscopic epifluorescence microscopy were selected for monitoring. All monitored vessels were 30–80 μm in diameter. Two to three vessels per mouse were selected and rolling cells were counted before and after antibody injection. The number of rolling cells before 4RA10 was normalized to 100% and the percent reduction after 4RA10 treatment was calculated.

Statistics. Statistical analyses for flow cytometry and inflammatory indices were performed using the two-tailed unpaired Student's *t* test. Data were expressed as mean and standard error of the mean. Statistical significance was set at $P < 0.05$.

Online supplemental material. Supplemental Videos 1 and 2 depict the interactions between CFSE-labeled PSGL-$1^{-/-}$ cells and intestinal endothelium before and after injection of mAb 4RA10; they are available at http://www.jem.org/cgi/content/full/jem.20052530/DC1.

We thank the Morphology and Immunology cores of the UVA Silvio Conte Digestive Diseases Research Center (i.e., Dr. R. Mize for evaluation of histological sections, M. Solga, and J. Lannigan for valuable discussions and assistance with flow cytometry, S. Hoang for expert assistance with immunohistochemistry); T. Deem for assistance with intravital microscopy; A. Bruce, J. Ho, and O. Castañón-Cervantes for technical assistance; and Dr. G. Kollias for providing the original TNFΔARE breeding pairs.

This work was supported by grants from the National Institutes of Health (nos. DK-57880 and DK-067254) and by a Harold Amos grant from the Robert Wood Johnson Foundation.

The authors have no conflicting financial interests.

Submitted: 21 December 2005
Accepted: 22 February 2006

REFERENCES

1. Davidson, A., and B. Diamond. 2001. Autoimmune diseases. *N. Engl. J. Med.* 345:340–350.
2. Longobardi, T., P. Jacobs, and C.N. Bernstein. 2003. Work losses related to inflammatory bowel disease in the United States: results from the National Health Interview Survey. *Am. J. Gastroenterol.* 98:1064–1072.
3. Podolsky, D.K. 1991. Inflammatory bowel disease (1). *N. Engl. J. Med.* 325:928–937.
4. Fiocchi, C. 1998. Inflammatory bowel disease: etiology and pathogenesis. *Gastroenterology*. 115:182–205.
5. Targan, S.R., S.B. Hanauer, S.J. van Deventer, L. Mayer, D.H. Present, T. Braakman, K.L. DeWoody, T.F. Schaible, and P.J. Rutgeerts. 1997. A short-term study of chimeric monoclonal antibody cA2 to tumor necrosis factor α for Crohn's disease. Crohn's Disease cA2 Study Group. *N. Engl. J. Med.* 337:1029–1035.
6. Sandborn, W.J., and S.R. Targan. 2002. Biologic therapy of inflammatory bowel disease. *Gastroenterology*. 122:1592–1608.
7. Springer, T.A. 1995. Traffic signals on endothelium for lymphocyte recirculation and leukocyte emigration. *Annu. Rev. Physiol.* 57:827–872.
8. Matsumoto, S., Y. Okabe, H. Setoyama, K. Takayama, J. Ohtsuka, H. Funahashi, A. Imaoka, Y. Okada, and Y. Umesaki. 1998. Inflammatory bowel disease-like enteritis and caecitis in a senescence accelerated mouse P1/Yit strain. *Gut.* 43:71–78.
9. Kosiewicz, M.M., C.C. Nast, A. Krishnan, J. Rivera-Nieves, C.A. Moskaluk, S. Matsumoto, K. Kozaiwa, and F. Cominelli. 2001.

Th1-type responses mediate spontaneous ileitis in a novel murine model of Crohn's disease. *J. Clin. Invest.* 107:695–702.
10. Rivera-Nieves, J., G. Bamias, A. Vidrich, M. Marini, T.T. Pizarro, M.J. McDuffie, C.A. Moskaluk, S.M. Cohn, and F. Cominelli. 2003. Emergence of perianal fistulizing disease in the SAMP1/YitFc mouse, a spontaneous model of chronic ileitis. *Gastroenterology.* 124:972–982.
11. Strober, W., K. Nakamura, and A. Kitani. 2001. The SAMP1/Yit mouse: another step closer to modeling human inflammatory bowel disease. *J. Clin. Invest.* 107:667–670.
12. Powrie, F. 1995. T cells in inflammatory bowel disease: protective and pathogenic roles. *Immunity.* 3:171–174.
13. Olson, T.S., G. Bamias, M. Naganuma, J. Rivera-Nieves, T.L. Burcin, W. Ross, M.A. Morris, T.T. Pizarro, P.B. Ernst, F. Cominelli, and K. Ley. 2004. Expanded B cell population blocks regulatory T cells and exacerbates ileitis in a murine model of Crohn disease. *J. Clin. Invest.* 114:389–398.
14. Kato, S., R. Hokari, K. Matsuzaki, A. Iwai, A. Kawaguchi, S. Nagao, T. Miyahara, K. Itoh, H. Ishii, and S. Miura. 2000. Amelioration of murine experimental colitis by inhibition of mucosal addressin cell adhesion molecule-1. *J. Pharmacol. Exp. Ther.* 295:183–189.
15. Ludviksson, B.R., W. Strober, R. Nishikomori, S.K. Hasan, and R.O. Ehrhardt. 1999. Administration of mAb against α E β 7 prevents and ameliorates immunization-induced colitis in IL-2−/− mice. *J. Immunol.* 162:4975–4982.
16. Picarella, D., P. Hurlbut, J. Rottman, X. Shi, E. Butcher, and D.J. Ringler. 1997. Monoclonal antibodies specific for β 7 integrin and mucosal addressin cell adhesion molecule-1 (MAdCAM-1) reduce inflammation in the colon of scid mice reconstituted with CD45RBhigh CD4+ T cells. *J. Immunol.* 158:2099–2106.
17. Podolsky, D.K., R. Lobb, N. King, C.D. Benjamin, B. Pepinsky, P. Sehgal, and M. deBeaumont. 1993. Attenuation of colitis in the cotton-top tamarin by anti-α 4 integrin monoclonal antibody. *J. Clin. Invest.* 92:372–380.
18. Burns, R.C., J. Rivera-Nieves, C.A. Moskaluk, S. Matsumoto, F. Cominelli, and K. Ley. 2001. Antibody blockade of ICAM-1 and VCAM-1 ameliorates inflammation in the SAMP-1/Yit adoptive transfer model of Crohn's disease in mice. *Gastroenterology.* 121:1428–1436.
19. Rivera-Nieves, J., T. Olson, G. Bamias, A. Bruce, M. Solga, R.F. Knight, S. Hoang, F. Cominelli, and K. Ley. 2005. L-selectin, α4 β1, and α4 β7 integrins participate in $CD4^+$ T cell recruitment to chronically inflamed small intestine. *J. Immunol.* 174:2343–2352.
20. Ghosh, S., E. Goldin, F.H. Gordon, H.A. Malchow, J. Rask-Madsen, P. Rutgeerts, P. Vyhnalek, Z. Zadorova, T. Palmer, and S. Donoghue. 2003. Natalizumab for active Crohn's disease. *N. Engl. J. Med.* 348:24–32.
21. von Andrian, U.H., and B. Engelhardt. 2003. α4 integrins as therapeutic targets in autoimmune disease. *N. Engl. J. Med.* 348:68–72.
22. Feagan, B.G., G.R. Greenberg, G. Wild, R.N. Fedorak, P. Pare, J.W. McDonald, R. Dube, A. Cohen, A.H. Steinhart, S. Landau, et al. 2005. Treatment of ulcerative colitis with a humanized antibody to the α4β7 integrin. *N. Engl. J. Med.* 352:2499–2507.
23. Sallusto, F., D. Lenig, R. Forster, M. Lipp, and A. Lanzavecchia. 1999. Two subsets of memory T lymphocytes with distinct homing potentials and effector functions. *Nature.* 401:708–712.
24. von Andrian, U.H., and C.R. Mackay. 2000. T-cell function and migration. Two sides of the same coin. *N. Engl. J. Med.* 343:1020–1034.
25. Hemmerich, S., E.C. Butcher, and S.D. Rosen. 1994. Sulfation-dependent recognition of high endothelial venules (HEV)-ligands by L-selectin and MECA 79, and adhesion-blocking monoclonal antibody. *J. Exp. Med.* 180:2219–2226.
26. Rosen, S.D. 1999. Endothelial ligands for L-selectin: from lymphocyte recirculation to allograft rejection. *Am. J. Pathol.* 155:1013–1020.
27. Butcher, E.C., M. Williams, K. Youngman, L. Rott, and M. Briskin. 1999. Lymphocyte trafficking and regional immunity. *Adv. Immunol.* 72:209–253.
28. Berg, E.L., L.M. McEvoy, C. Berlin, R.F. Bargatze, and E.C. Butcher. 1993. L-selectin-mediated lymphocyte rolling on MAdCAM-1. *Nature.* 366:695–698.
29. McEver, R.P., and R.D. Cummings. 1997. Role of PSGL-1 binding to selectins in leukocyte recruitment. *J. Clin. Invest.* 100:S97–S103.
30. Hirata, T., G. Merrill-Skoloff, M. Aab, J. Yang, B.C. Furie, and B. Furie. 2000. P-Selectin glycoprotein ligand 1 (PSGL-1) is a physiological ligand for E-selectin in mediating T helper 1 lymphocyte migration. *J. Exp. Med.* 192:1669–1676.
31. Xia, L., M. Sperandio, T. Yago, J.M. McDaniel, R.D. Cummings, S. Pearson-White, K. Ley, and R.P. McEver. 2002. P-selectin glycoprotein ligand-1-deficient mice have impaired leukocyte tethering to E-selectin under flow. *J. Clin. Invest.* 109:939–950.
32. Bargatze, R.F., M.A. Jutila, and E.C. Butcher. 1995. Distinct roles of L-selectin and integrins α4 β7 and LFA-1 in lymphocyte homing to Peyer's patch-HEV in situ: the multistep model confirmed and refined. *Immunity.* 3:99–108.
33. Thatte, A., S. Ficarro, K.R. Snapp, M.K. Wild, D. Vestweber, D.F. Hunt, and K.F. Ley. 2002. Binding of function-blocking mAbs to mouse and human P-selectin glycoprotein ligand-1 peptides with and without tyrosine sulfation. *J. Leukoc. Biol.* 72:470–477.
34. Inoue, T., Y. Tsuzuki, K. Matsuzaki, H. Matsunaga, J. Miyazaki, R. Hokari, Y. Okada, A. Kawaguchi, S. Nagao, K. Itoh, et al. 2005. Blockade of PSGL-1 attenuates $CD14^+$ monocytic cell recruitment in intestinal mucosa and ameliorates ileitis in SAMP1/Yit mice. *J. Leukoc. Biol.* 77:287–295.
35. Kozaiwa, K., K. Sugawara, M.F. Smith Jr., V. Carl, V. Yamschikov, B. Belyea, S.B. McEwen, C.A. Moskaluk, T.T. Pizarro, F. Cominelli, and M. McDuffie. 2003. Identification of a quantitative trait locus for ileitis in a spontaneous mouse model of Crohn's disease: SAMP1/YitFc. *Gastroenterology.* 125:477–490.
36. Sperandio, M., M.L. Smith, S.B. Forlow, T.S. Olson, L. Xia, R.P. McEver, and K. Ley. 2003. P-selectin glycoprotein ligand-1 mediates L-selectin–dependent leukocyte rolling in venules. *J. Exp. Med.* 197:1355–1363.
37. Collins, R.G., U. Jung, M. Ramirez, D.C. Bullard, M.J. Hicks, C.W. Smith, K. Ley, and A.L. Beaudet. 2001. Dermal and pulmonary inflammatory disease in E-selectin and P-selectin double-null mice is reduced in triple-selectin-null mice. *Blood.* 98:727–735.
38. M'Rini, C., G. Cheng, C. Schweitzer, L.L. Cavanagh, R.T. Palframan, T.R. Mempel, R.A. Warnock, J.B. Lowe, E.J. Quackenbush, and U.H. von Andrian. 2003. A novel endothelial L-selectin ligand activity in lymph node medulla that is regulated by α(1,3)-fucosyltransferase-IV. *J. Exp. Med.* 198:1301–1312.
39. Kontoyiannis, D., M. Pasparakis, T.T. Pizarro, F. Cominelli, and G. Kollias. 1999. Impaired on/off regulation of TNF biosynthesis in mice lacking TNF AU-rich elements: implications for joint and gut-associated immunopathologies. *Immunity.* 10:387–398.
40. Fabien, N., I. Bergerot, J. Orgiazzi, and C. Thivolet. 1996. Lymphocyte function associated antigen-1, integrin α4, and L-selectin mediate T-cell homing to the pancreas in the model of adoptive transfer of diabetes in NOD mice. *Diabetes.* 45:1181–1186.
41. Hanninen, A., C. Taylor, P.R. Streeter, L.S. Stark, J.M. Sarte, J.A. Shizuru, O. Simell, and S.A. Michie. 1993. Vascular addressins are induced on islet vessels during insulitis in nonobese diabetic mice and are involved in lymphoid cell binding to islet endothelium. *J. Clin. Invest.* 92:2509–2515.
42. Mikulowska-Mennis, A., B. Xu, J.M. Berberian, and S.A. Michie. 2001. Lymphocyte migration to inflamed lacrimal glands is mediated by vascular cell adhesion molecule-1/ α(4)β(1) integrin, peripheral node addressin/l-selectin, and lymphocyte function-associated antigen-1 adhesion pathways. *Am. J. Pathol.* 159:671–681.
43. Sikorski, E.E., R. Hallmann, E.L. Berg, and E.C. Butcher. 1993. The Peyer's patch high endothelial receptor for lymphocytes, the mucosal vascular addressin, is induced on a murine endothelial cell line by tumor necrosis factor-α and IL- 1. *J. Immunol.* 151:5239–5250.
44. Briskin, M., D. Winsor-Hines, A. Shyjan, N. Cochran, S. Bloom, J. Wilson, L.M. McEvoy, E.C. Butcher, N. Kassam, C.R. Mackay, et al. 1997. Human mucosal addressin cell adhesion molecule-1 is preferentially expressed in intestinal tract and associated lymphoid tissue. *Am. J. Pathol.* 151:97–110.
45. Laszik, Z., P.J. Jansen, R.D. Cummings, T.F. Tedder, R.P. McEver, and K.L. Moore. 1996. P-selectin glycoprotein ligand-1 is broadly expressed in cells of myeloid, lymphoid, and dendritic lineage and in some nonhematopoietic cells. *Blood.* 88:3010–3021.

46. Austrup, F., D. Vestweber, E. Borges, M. Lohning, R. Brauer, U. Herz, H. Renz, R. Hallmann, A. Scheffold, A. Radbruch, and A. Hamann. 1997. P- and E-selectin mediate recruitment of T-helper-1 but not T- helper-2 cells into inflammed tissues. *Nature*. 385:81–83.
47. Borges, E., W. Tietz, M. Steegmaier, T. Moll, R. Hallmann, A. Hamann, and D. Vestweber. 1997. P-selectin glycoprotein ligand-1 (PSGL-1) on T helper 1 but not on T helper 2 cells binds to P-selectin and supports migration into inflamed skin. *J. Exp. Med.* 185:573–578.
48. Ley, K., and G.S. Kansas. 2004. Selectins in T-cell recruitment to non-lymphoid tissues and sites of inflammation. *Nat. Rev. Immunol.* 4:325–335.
49. Majuri, M.L., M. Pinola, R. Niemela, S. Tiisala, J. Natunen, O. Renkonen, and R. Renkonen. 1994. α2,3-sialyl and α1,3-fucosyltransferase-dependent synthesis of sialyl Lewis x, an essential oligosaccharide present on L-selectin counterreceptors, in cultured endothelial cells. *Eur. J. Immunol.* 24:3205–3210.
50. Huo, Y., A. Schober, S.B. Forlow, D.F. Smith, M.C. Hyman, S. Jung, D.R. Littman, C. Weber, and K. Ley. 2003. Circulating activated platelets exacerbate atherosclerosis in mice deficient in apolipoprotein E. *Nat. Med.* 9:61–67.
51. Mori, M., J.W. Salter, T. Vowinkel, C.F. Krieglstein, K.Y. Stokes, and D.N. Granger. 2005. Molecular determinants of the prothrombogenic phenotype assumed by inflamed colonic venules. *Am. J. Physiol. Gastrointest. Liver Physiol.* 288:G920–G926.
52. Chen, S.C., C.C. Huang, C.L. Chien, C.J. Jeng, H.T. Su, E. Chiang, M.R. Liu, C.H. Wu, C.N. Chang, and R.H. Lin. 2004. Cross-linking of P-selectin glycoprotein ligand-1 induces death of activated T cells. *Blood.* 104:3233–3242.
53. Hamann, A., D.P. Andrew, D. Jablonski-Westrich, B. Holzmann, and E.C. Butcher. 1994. Role of α4-integrins in lymphocyte homing to mucosal tissues in vivo. *J. Immunol.* 152:3282–3293.
54. Kunkel, E.J., C.L. Ramos, D.A. Steeber, W. Muller, N. Wagner, T.F. Tedder, and K. Ley. 1998. The roles of L-selectin, β7 integrins, and P-selectin in leukocyte rolling and adhesion in high endothelial venules of Peyer's patches. *J. Immunol.* 161:2449–2456.